Solitaire and Gemini Metallocene Porphyrazines

Sarah L. J. Michel,[†] David P. Goldberg,[†,§] Charlotte Stern,[†] Anthony G. M. Barrett,*[,‡] and Brian M. Hoffman*[,†]

Contribution from the Departments of Chemistry, Northwestern University, Evanston, Illinois 60208, and Imperial College of Science, Technology and Medicine, London, U.K. SW7 2AY

Received October 17, 2000

Abstract: We report the synthesis and physical characterization of a series of peripherally functionalized porphyrazines (pzs) of the forms H_2[pz(**A;B**$_3$)] and *trans*-H_2[pz(**A**$_2$**;B**$_2$)], where **A** is a dithiolene chelate of molybdocene or vanadocene and **B** is a solublizing group. The precursor pz's **8** and **9**, of the form H_2[pz-(**A;B**$_3$)], where **A** = (4-(butyloxycarbonyl)-*S*-benzyl)$_2$ and **B** = di-*tert*-butylphenyl (**8**) or di-*n*-propyl (**9**), have been prepared, deprotected, and peripherally metalated with molybdocene and vanadocene to form **1**(**Mo^{IV}**) and **1**(**V^{IV}**), prepared from **8**, and **2**(**Mo^{IV}**) from **9**, respectively. Likewise, the protected *trans*-H_2[pz(**A**$_2$**;B**$_2$)], where **A** = (*S*-benzyl)$_2$ and **B** = 3,6-butyloxybenzene (**12**) or **A** = (*S*-benzyl)$_2$ and **B** = (*tert*-butylphenyl)$_2$ (**13**), have been prepared and peripherally metalated with molybdocene and vanadocene to give the trans dinuclear complexes, **3**(**Mo^{IV},Mo^{IV}**), **3**(**V^{IV},V^{IV}**) (from **12**), and **4**(**V^{IV},V^{IV}**) (from **13**). A crystal structure of the trans vanadocene pz **4**(**V^{IV},V^{IV}**) is presented; the distance between the two vanadium atoms is 14.5 Å. The molybdocene-appended pz's are highly redox active and exhibit cyclic voltammograms that are more than just the sum of the metallocene and the parent pz's. Chemical oxidation with $FcPF_6$ gives the Mo^V species **1**(**Mo^{V}**), **2**(**Mo^{V}**), **3**(**Mo^{V},Mo^{IV}**), and **3**(**Mo^{V},Mo^{V}**). Their EPR spectra are indicative of extensive delocalization from the Mo^V into the dithiolato-pz. The EPR spectrum of the mononuclear paramagnetic vanadocene pz, **1**(**V^{IV}**), shows an expected 8-line pattern for an $S = 2$ system with hyperfine coupling to a single ^{51}V ($I = {}^7/_2$) nucleus, but the dinuclear vanadocene pz's, **3**(**V^{IV},V^{IV}**) and **4**(**V^{IV},V^{IV}**), exhibit a striking 15-line pattern of the same breadth from the $S = 1$ state formed by exchange coupling between the $S = 2$ vanadium centers of a dinuclear complex. Thus, the porphyrazine macrocycle is capable of mediating magnetic exchange interactions between metal ions bound to the periphery, separated by 14.5 Å.

Introduction

Porphyrazines (pzs), or tetraazaporphyrins, are porphyrin variants in which the meso positions have nitrogens, not C−H.[1] Not only does this difference give pz's physiochemical properties intrinsically different from those of the porphyrins, but the pz synthetic route also allows for the ready preparation of macrocycles which have heteroatoms directly fused at the β-position of the pyrroles.[2] As part of an effort to prepare heteroatom-functionalized pz's, we have developed procedures for the cocyclization of two different dinitriles to generate porphyrazines of the form M[pz(**A**$_n$**;B**$_{4-n}$)], $n = 1, 2, 4$, where **A** is a dithiolene moiety and **B** is a solubilizing group,[3−6] and have used them to bind metal ion "caps" to the periphery of the pz.[3−5,7]

Recently, we reported the covalent attachment of a single molybdocene to a dithiolene binding site on the pz periphery[7] and discovered that this complex exhibited physical and electrochemical properties that were more than just the sum of the properties of the porphyrazine and molybdocene dithiolene fragments. Here, we report the synthesis and physical characterization of a series of metallocene-substituted porphyrazines of the form H_2[pz(**A;B**$_3$)] and *trans*-H_2[pz(**A**$_2$**;B**$_2$)], where the **A** functionality is a dithiolene chelate used to bind redox-active molybdocene and paramagnetic vanadocene units, and the **B** functionality is designed to impart solubility in organic solvents to the pz (Schemes 1 and 2). Macrocycles peripherally chelated with molybdocene are highly redox active, and the oxidized Mo^V forms exhibit EPR spectra indicative of extensive delocalization from the Mo^V into the dithiolato-pz. The H_2[pz-(**A**$_2$**;B**$_2$)], **A** = S_2VCp_2 (Scheme 2, **3**(**V^{IV},V^{IV}**) and **4**(**V^{IV},V^{IV}**))

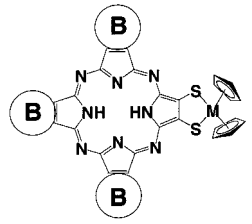

1(M); B = (4-*t*-butyl phenyl)$_2$
2(M); B = (*n*-propyl)$_2$

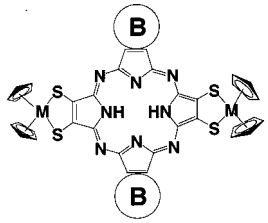

3(M); B = 3,6 butyloxybenzene
4(M); B = (4-*t*-butyl phenyl)$_2$

[†] Northwestern University.
[‡] Imperial College of Science, Technology and Medicine.
[§] Current address: Department of Chemistry, The Johns Hopkins University, Baltimore, MD 21218.

(1) Linstead, R. P.; Whalley, M. *J. Chem. Soc. (London)* **1952**, 4839−4844.
(2) Michel, S. L. J.; Baum, S.; Barrett, A. G. M.; Hoffman, B. M. In *Progress in Inorganic Chemistry*; Wiley: New York, 2001.

10.1021/ja003702x CCC: $20.00
Published on Web 04/25/2001

Scheme 1. Preparation and Peripheral Metalation of Solitaire Porphyrazines[a]

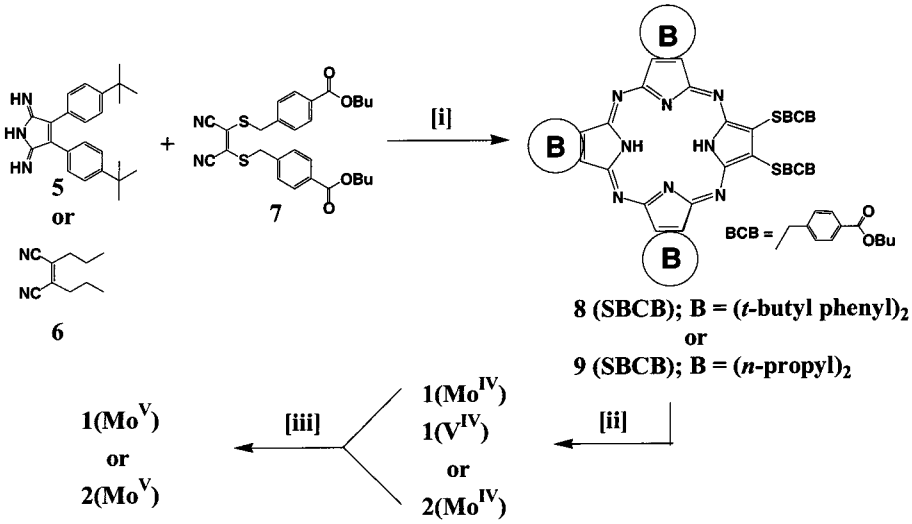

[a] Conditions: [i] (a) $Mg(OBu)_2$, BuOH, reflux; (b) TFA, NH_4OH. [ii] (a) Na, NH_3(l), THF, −78 °C; (b) Cp_2MCl_2, M = Mo, V. [iii] $FcPF_6$, CH_2Cl_2.

Scheme 2. Preparation and Peripheral Metalation of Solitaire Porphyrazines[a]

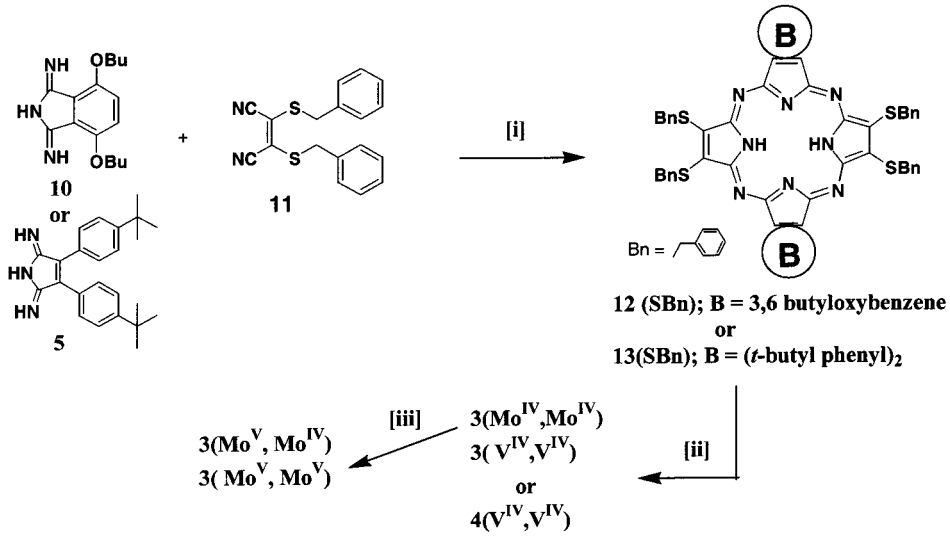

[a] Conditions: [i] (a) $Mg(OBu)_2$, BuOH, 100 °C; (b) TFA, NH_4OH. [ii] (a) Na, NH_3(l), THF, −78 °C; (b) Cp_2MCl_2, M = Mo, V. [iii] $FcPF_6$, CH_2Cl_2/acetone.

compounds exhibit triplet EPR spectra, demonstrating the presence of exchange coupling between two peripheral vanadium atoms separated by over 14.5 Å.

Results

Synthesis of the "Solitaire" Porphyrazines 1 and 2. The preparation of the soluble *solitaire* porphyrazines, **1** and **2**, which are of the form H_2[pz(**A**;**B**$_3$)], begins with the mixed condensation of 4-(butyloxycarbonyl)benzyl-protected dithiomaleonitrile, $(BCB)_2$mnt (**7**),[4] with either bis(4-*tert*-butylphenyl)pyrroline (**5**)[8] or dipropylmaleonitrile (**6**)[9] (Scheme 1) under Linstead magnesium ion template conditions.[1,10] The use of the two reactants, bis(4-*tert*-butylphenyl)pyrroline (**5**) and dipropylmaleonitrile (**6**) was part of an effort to optimize the **B** solubilizing groups. Previously, we had prepared norphthalocyanine pz's, where the **B** groups are fused benzene rings, but these pz's have limited solubility in organic solvents, and this hindered the preparation of metallocene-substituted pz's. The use of **5** and **6** led to porphyrazines **8** (16%) and **9** (12%), which are fully soluble in common organic solvents ($CHCl_3$, CH_2Cl_2, etc.). In addition, the desired cyclization products, **8** and **9**, can be easily separated from the other isomers by routine chromatographic methods (silica gel, CH_2Cl_2, or CH_2Cl_2/MeOH eluant) because the differences in polarity between the **A** and **B** groups imparts a

(3) Baumann, T. F.; Sibert, J. W.; Olmstead, M. M.; Barrett, A. G. M.; Hoffman, B. M. *J. Am. Chem. Soc.* **1994**, *116*, 2639−2640.
(4) Baumann, T. F.; Nasir, M. S.; Sibert, J. W.; White, A. J. P.; Olmstead, M. M.; Williams, D. J.; Barrett, A. G. M.; Hoffman, B. M. *J. Am. Chem. Soc.* **1996**, *118*, 10479−10486.
(5) Sibert, J. W.; Baumann, T. F.; Williams, D. J.; White, A. J. P.; Barrett, A. G. M.; Hoffman, B. M. *J. Am. Chem. Soc.* **1996**, *118*, 10487−10493.
(6) Forsyth, T. P.; Williams, D. B. G.; Montalban, A. G.; Stern, C. L.; Barrett, A. G. M.; Hoffman, B. M. *J. Org. Chem.* **1998**, *63*, 331−336.
(7) Goldberg, D. P.; Michel, S. L. J.; White, A. J. P.; Williams, D. J.; Barrett, A. G. M.; Hoffman, B. M. *Inorg. Chem.* **1998**, *37*, 2100−2101.
(8) Baumann, T. F.; Barrett, A. G. M.; Hoffman, B. M. *Inorg. Chem.* **1997**, *36*, 5661−5665.
(9) Lange, S. J.; Nie, H.; Stern, C. L.; Barrett, A. G. M.; Hoffman, B. M. *Inorg. Chem.* **1998**, *37*, 6435−6443.
(10) Greene, T. W.; Wuts, P. G. M. *Protective Groups in Organic Synthesis*, 2nd ed.; John Wiley and Sons: New York, 1991.

large difference in the polarity moments of the various cyclization products (Scheme 1).

Using Schlenck techniques, the BCB protecting group was removed from either pz **8** or **9** using sodium and ammonia,[10] and the resultant dithiolato pz, $H_2[pz(S_2^{2-};\mathbf{B_3})]$, where **B** = (4-*tert*-butylphenyl)$_2$ (**8a**) or (*n*-propyl)$_2$ (**9a**), was reacted, *in situ*, with Cp_2MCl_2 (M = Mo, V) to form **1**(**Mo^{IV}**), **1**(**V^{IV}**), and **2**(**Mo^{IV}**) (Scheme 1). Porphyrazines **1**(**Mo^{IV}**) and **2**(**Mo^{IV}**) are air-stable and freely soluble in most organic solvents and were purified by column chromatography; **1**(**V^{IV}**) is air-sensitive, so purification by column chromatography was carried out in an inert atmosphere glovebox.

Synthesis of the Trans "Gemini" Porphyrazines 3 and 4. The soluble *trans*-$H_2[pz(S\text{-benzyl})_2;\mathbf{B_2}]$, where **B** = 3,6-butyloxybenzene (**12**), was prepared by cyclizing bis(benzylthio)maleonitrile (**11**) with 4,7-bis(butyloxy)-1,3-diiminoisoindoline (**10**) (Scheme 2). The yield of **12** is a function of the ratio of the two cyclization partners and the relative reactivity of the two components. Bis(benzylthio)maleonitrile (**11**) is much more reactive than the diiminoisoindoline, **10**, and the latter reacts only with the cocyclization partner under the conditions employed, to give mainly **12**, which was purified by column chromatography. The *S*-benzyl protecting groups of **12** were removed with sodium and ammonia, and the resultant bis-dithiolato-pz, was reacted in situ with Cp_2MCl_2 (M = Mo, V) to give **3**(**Mo^{IV},Mo^{IV}**) and **3**(**V^{IV},V^{IV}**). The *trans*-$H_2[pz(S\text{-benzyl})_2;\mathbf{B_2}]$, where **B** = (4-*tert*-butylphenyl)$_2$ (**13**), is a minor product of the cocyclization of bis(benzylthio)maleonitrile (**11**) with bis(4-*tert*-butylphenyl)pyrroline (**5**), and its yield could not be improved appreciably. Nonetheless, **13** was deprotected and peripherally chelated with vanadocene to form **4**(**V^{IV},V^{IV}**) via the same route. Perversely, crystals were obtained only for **4**(**V^{IV},V^{IV}**) and not for **3**(**Mo^{IV},Mo^{IV}**) or **3**(**V^{IV},V^{IV}**).

X-ray Structure of 4(V^{IV},V^{IV}). Dark green, platelike crystals of **4**(**V^{IV},V^{IV}**) were grown from an acetone/MeOH solution. Crystallographic characterization revealed that **4**(**V^{IV},V^{IV}**) stacks in a typical herringbone fashion. Figure 1 shows an ORTEP diagram of the complex; the pertinent parameters for the data collection and structure determination are given in Table 1. As expected, the Cp_2V units are coordinated to two thiolates of a pyrrole, like the analogous vanadium benzenedithiolate.[11] The macrocycle lies on an inversion center, and the imposed symmetry causes the two S_2VCp_2 units to have identical bond distances and angles. The average V−S bond distance of 2.438 Å matches the values reported for similar vanadium dithiolenes[11] and is 0.036 Å shorter than the Mo−S bond distances for the corresponding molybdenum porphyrazine complex **1**(**Mo^{IV}**)[7] because of the smaller ionic radius of vanadium. The average V−Cp (centroid) distance of 2.299 Å is also similar to the values reported for other vanadocene structures.[11] The C−S distances, 1.725 Å, are consistent with single bonds, as for **1**(**Mo^{IV}**).[7] Likewise, the C_β−C_β−S average bond angle of 125(2)° matches that found for **1**(**Mo^{IV}**)[7] as well as the analogous angles previously reported for Ni, Pt, and Pt *cis*-diphosphine "star" porphyrazines.[12−14]

The dihedral angle between the VS_2 plane and the plane of the porphyrazine is approximately 30°; because of the inversion center, one of the vanadium atoms lies above the pz ring plane while the other lies below. Such a tilt of the metallocene unit in relation to the dithiolene ligand plane has been observed in other 17-electron, d^1 dithiolate MCp_2 complexes.[15] Fourmigué et al. suggested that this tilted orientation allows for better overlap between the 17-electron metal center and the filled p orbitals on the sulfur, which tends to make the metal center less electron deficient.[16] In support of this idea, the five-membered chelate ring for **1**(**Mo^{IV}**),[7] which is an 18-electron d^2 system, is essentially planar.

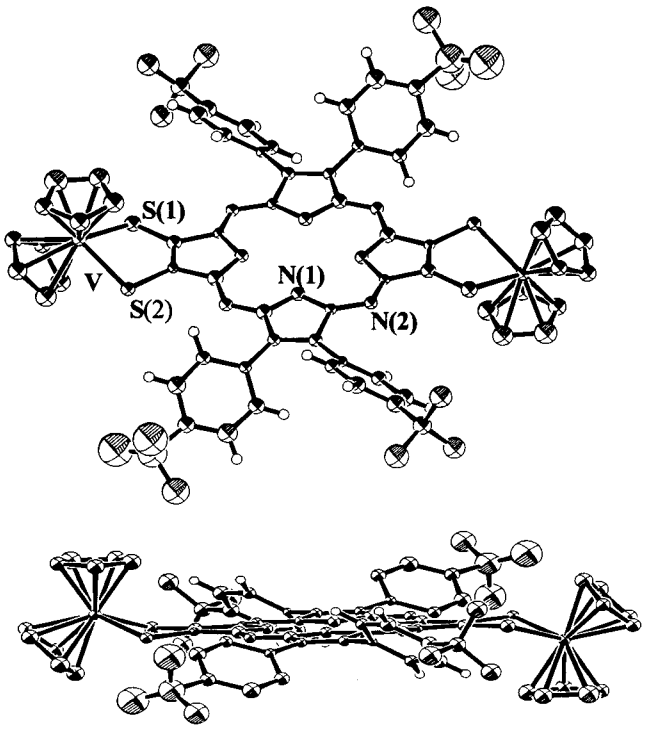

Figure 1. Two perspectives of the molecular structure of the divanadium pz **4**(**V^{IV},V^{IV}**). For clarity, the heteroatoms have been labeled, and the hydrogen atoms have been omitted.

Table 1. Crystal Data and Structure Refinement for **4**(**V^{IV},V^{IV}**)

empirical formula	$V_2C_{86}H_{88}N_8O_6S_4$
formula weight	1559.81
crystal system	monoclinic
space group	*P*21/*c* (No. 14)
crystal color, habit	green, rectangles
crystal dimensions	0.177 × 0.17 × 0.20 mm
lattice parameters	*a* = 13.4103 Å
	b = 12.8078 Å
	c = 24.4431 Å
	β = 97.4744°
	V = 4162.58789(4) Å^3
temperature	−120 ± 1 °C
Z value	2
residuals: R1; wR2	0.143; 0.239
goodness-of-fit indicator	1.75

Electrochemistry. The cyclic voltammograms of **8** and **9** show two reversible ring reductions, at $E_{1/2}$ = −1045 (Pz/Pz$^-$) and −1376 mV (Pz$^-$/Pz^{2-}) for **8** (Figure 2) and at $E_{1/2}$ = −1235 (Pz/Pz$^-$) and −1597 mV (Pz$^-$/Pz^{2-}) for **9**, plus an irreversible ring oxidation at $E_{1/2}$ = 839 mV for **8** (Pz$^+$/Pz) and at $E_{1/2}$ = 722 mV for **9** (Pz$^+$/Pz) (ref vs Fc$^+$/Fc) (Table 2). The cyclic voltammogram for the trans pz, **12**, shows one reversible ring reduction, at $E_{1/2}$ = −1018 mV (Pz/Pz$^-$), and a quasi-reversible

(11) Stephan, D. W. *Inorg. Chem.* **1992**, *31*, 4128−4223.
(12) Velázquez, C. S.; Baumann, T. F.; Olmstead, M. M.; Hope, H.; Barrett, A. G. M.; Hoffman, B. M. *J. Am. Chem. Soc.* **1993**, *115*, 9997−10003.
(13) Velázquez, C. S.; Fox, G. A.; Broderick, W. E.; Andersen, K. A.; Anderson, O. P.; Barrett, A. G. M.; Hoffman, B. M. *J. Am. Chem. Soc.* **1992**, *114*, 7416−7424.
(14) Velazquez, C. S.; Broderick, W. E.; Sabat, M.; Barrett, A. G. M.; Hoffman, B. M. *J. Am. Chem. Soc.* **1990**, *112*, 7408−7410.
(15) Fourmigué, M. *Coord. Chem. Rev.* **1998**, *178−180*, 823−864.
(16) Fourmigué, M.; Lenoir, C.; Coulon, C.; Guyon, F.; Amaudrut, J. *Inorg. Chem.* **1995**, *34*, 4979−4985.

Table 2. Comparison of Half-Wave Potentials (mV vs Fc^+/Fc)

compound	Pz^{2+}/Pz	Pz^+/Pz	Mo^{VI}/Mo^V	Mo^V/MO^{IV}	Pz/Pz^-	Pz^-/Pz^{2-}
8		839 (irrev)			−1045 (122)	−1376 (186)
9		722 (irrev)			−1235 (106)	−1597 (118)
1(Mo^{IV})		1060 (67)	522 (116)	−132 (76)	−1290 (68)	−1530 (68)
2(Mo^{IV})		1060 (194)	460 (108)	−158 (80)	−1310 (76)	−1770 (102)
12	772 (88)	355 (110)			−1018 (96)	−1344 (228)
3(Mo^{IV},Mo^{IV})				−38 (76)	−1503 (74)	
1:3 Pc					−1230	−1590
octa-*S*-benzyl-Pz					−850	−1190

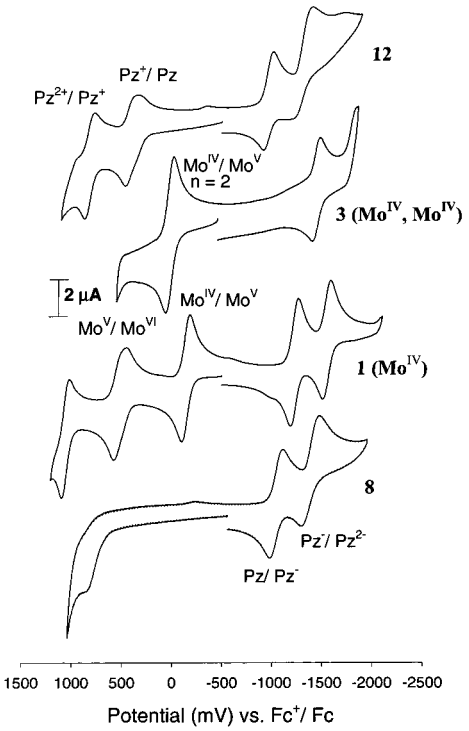

Figure 2. Cyclic voltammograms for **8**, **1**(**Mo^{IV}**), **3**(**Mo^{IV}**,**Mo^{IV}**), and **12** in CH_2Cl_2 with 0.1 M $TBAPF_6$, referenced versus Fc^+/Fc.

couple at $E_{1/2} = -1344$ mV (Pz^-/Pz^{2-}), but also two fully reversible ring oxidations, at $E_{1/2} = 335$ (Pz^+/Pz) and 772 mV (Pz^{2+}/Pz^+) (Figure 2). Although the number of **A** and **B** groups and the nature of the **B** groups differ for these three porphyrazines, these differences do not appear to affect the ring reductions, which are observed at approximately the same potentials. In contrast, **8** and **9**, which are of the form H_2[pz-(**A**;**B**$_3$)], show only a single, irreversible ring oxidation, while the trans pz, **12**, exhibits both a reversible and a quasi-reversible ring oxidation; this suggests that the oxidation potentials are more sensitive to changes at the periphery, although correlations are not obvious.

The peripheral metalation of **8** with molybdocene to form **1**(**Mo^{IV}**) produces a dramatically altered cyclic voltammogram in which five reversible waves are observed, two reductions and three oxidations (Figure 2). The first oxidation, at $E_{1/2} = -132$ mV, is typical of a Mo^V/Mo^{IV} couple,[15,17] but the reversible Mo^{VI}/Mo^V couple, seen as the second oxidation at $E_{1/2} = 522$ mV, is a rarity for this coordination environment.[15] The two ring reductions are shifted negative by as much as 250 mV to $E_{1/2} = -1290$ and -1530 mV, consistent with the Cp_2-Mo group acting as an electron-donating unit which changes the redox properties of the entire porphyrazine π-system. In contrast, the Pz^+/Pz couple is shifted positive by ~300 mV, to $E_{1/2} = +1060$ mV, by the addition of the metallocene unit, yet has been made reversible. (Note: Although other physical data show significant electronic delocalization between the metallocene fragment and the pz ring, the positive shift in the ring oxidation (Pz^+/Pz couple) must include charge effects resulting from the fact that the ring is oxidized from the Mo^{VI}pz species, which is a dication.) Thus, the molybdocene unit can act as both an electron-accepting and an electron-donating partner toward the porphyrazine. These same changes are observed for **2**(**Mo^{IV}**), whose specific oxidation potentials are given in Table 2.

The peripheral metalation of the trans pz, **12**, also results in dramatically altered electrochemistry. The first oxidation of **3**(**Mo^{IV}**,**Mo^{IV}**) (Figure 2), at $E_{1/2} = -38$ mV, is attributed to $Mo^{V/IV}$, and its height, 4.5 μA, is twice that of the ring reduction at $E_{1/2} = -1503$ mV (Pz/Pz^-), 2.2 μA (and the internal ferrocene standard), indicating that the two $MoCp_2$ units undergo the $Mo^{IV/V}$ process at essentially the same potential.[18] The peaks have equal widths, ΔE, indicating that within the precision of the measurements the redox processes for the two metal centers at 14.5 Å separation are essentially independent. Only one ring reduction is observed, centered at $E_{1/2} = -1503$ mV (Pz/Pz^-). This is 485 mV more negative than the first ring reduction observed for the parent pz, **12**. This negative shift in potential of the ring reduction is consistent with the Cp_2Mo group acting as an electron donor to the porphyrazine π-system. This shift is almost double the one observed for **1**(**Mo^{IV}**), consistent with double the number of molybdocene units (2) chelated. In addition, nonreversible redox processes occur beyond +600 mV, which limits the potential range of the scan. No ring oxidations are observed within the potential scanned (Figure 2).

Electronic Spectra. Figure 3 compares the optical spectra of **8**, **1**(**Mo^{IV}**), **1**(**Mo^{V}**), and **1**(**V^{IV}**). Pz **8** has idealized C_{2v} symmetry and a split Q-band, $\lambda = 608$ and 678 nm. The presence of $MoCp_2$ in **1**(**Mo^{IV}**) rather than the two thioethers of **8** causes the Q-band to coalesce to a single peak, $\lambda = 620$, a phenomenon that we previously reported for the peripheral metalation of norphthalocyanine-appended pz's with Ni, Pt, and Pd *cis*-diphosphine units,[4] and which may be due to an extension of the pz π-system into the peripheral metal chelate ring mediated by the bridging sulfur atoms.

The electrochemical data indicate that **1**(**Mo^{IV}**) can be oxidized to **1**(**Mo^{V}**)PF_6 ($E_{1/2} = -132$) by addition of ferrocenium hexafluorophophate ($E_{1/2} = 0$). This oxidation causes the single Q-band of **1**(**Mo^{IV}**) at $\lambda = 620$ to split into two peaks, $Q_y = 622$ nm and $Q_x = 672$ nm for **1**(**Mo^{V}**). Similarly, for **2**(**Mo^{IV}**) ($E_{1/2} = -158$), the single Q-band at $\lambda = 637$ nm splits into two peaks at $Q_y = 601$ nm and $Q_x = 627$ nm upon oxidation to **2**(**Mo^{V}**). These oxidations are fully reversible: addition of cobaltocene to **1**(**Mo^{V}**) and **2**(**Mo^{V}**) regenerates **1**(**Mo^{IV}**) and **2**(**Mo^{IV}**). The vanadocene pz, **1**(**V^{IV}**), which is isoelectronic with the one-electron oxidized molybdocene pz, **1**(**Mo^{V}**), also exhibits

(17) Hsu, J. K.; Bonangelino, C. J.; Kaiwar, S. P.; Boggs, C. M.; Fettinger, J. C.; Pilato, R. S. *Inorg. Chem.* **1996**, *35*, 4743−4751.

(18) Bard, A. J.; Faulkner, L. R. *Electrochemical Methods*; Wiley: New York, 1980.

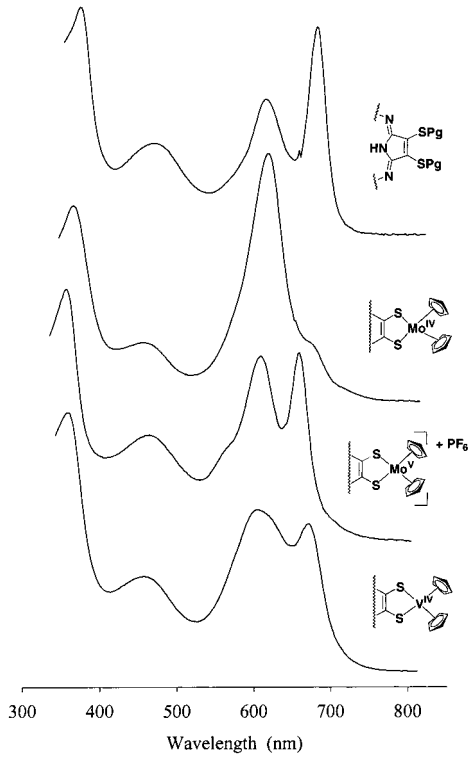

Figure 3. Absorption spectra of complexes **8**, **1**(**Mo**^{IV}), **1**(**Mo**^{V}), and **1**(**V**^{IV}) (CH_2Cl_2).

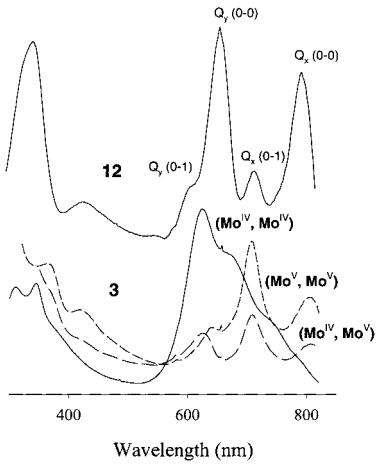

Figure 4. Absorption spectra of complexes **12** (top), **3**(**Mo**^{IV},**Mo**^{IV}), **3**(**Mo**^{V},**Mo**^{IV}), and **3**(**Mo**^{V},**Mo**^{V}) (CH_2Cl_2).

a split Q-band, with measured absorbances of $\lambda = 609$ and 684 nm.

The two 3,6-butyloxybenzene groups of the trans porphyrazine, **12**, enhance the Q-band red-shift and splitting: $Q_x = 796$ nm and $Q_y = 656$ nm, as reported previously (Figure 4).[6,19,20] In addition, a small peak is observed at 720 nm, which we tentatively assign as a Q_x("0 → 1") transition, corresponding to a vibrational frequency of 1326 cm^{-1} and likely attributable to ring vibrational modes. Peripheral metalation with molybdocene drastically alters the breadth and intensity of features in the Q-band region, although the Q_x and Q_y features and their vibrational partners still can be discerned. The one-electron and two-electron oxidations to **3**(**Mo**^{V},**Mo**^{IV}) and **3**(**Mo**^{V},**Mo**^{V})

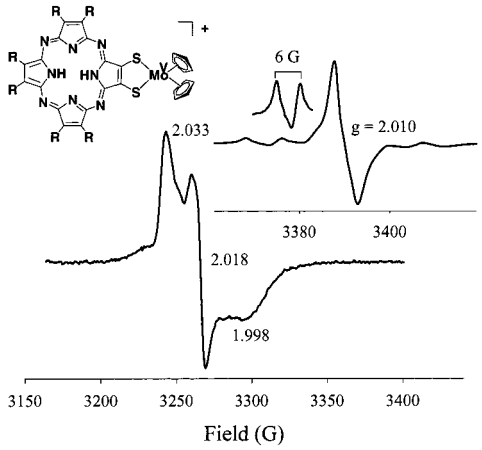

Figure 5. X-band, 77 K, EPR spectrum of **1**(**Mo**^{V}) in $CHCl_3$/toluene (50:50), mod. amp. = 2.5 G. Inset: X-band, 298 K, EPR spectrum of **1**(**Mo**^{V}), mod. amp. = 5.0 G.

Table 3. Comparison of EPR Parameters for Molybdocene Dithiolene Systems

compound	$\langle g \rangle$	A_{iso} (MHz)	reference
$[Cp_2MoCl_2]^+$	1.999	105	
$[Cp_2Mo(O_2CPh)_2]^+$	1.982	111	21
$[Cp_2MoMeTDT]^+$ [a]	2.009	50	
1(**MO**^{V})$^+$	2.010	22	this work
2(**MO**^{V})$^+$	2.010	22	this work

[a] TDT = $[MeC_6H_4S_2]^{2-}$.

($E_{1/2} = -38$ mV) sharpen the absorbance peaks, although again they appear to occur at essentially the same wavelengths as for the trans pz, **12**.

Electron Paramagnetic Resonance Spectroscopy.

(i) Molybdocene pz's. The room-temperature and frozen-solution X-band EPR spectra of **1**(**Mo**^{V}) in CH_2Cl_2/*i*-PrOH are shown in Figure 5. The room-temperature spectrum (inset) shows a singlet centered at $g = 2.012$ attributable to the molybdenum species with spinless Mo ($I = 0$, 74.5%). In addition, the spectrum shows the four outer peaks of a lower intensity sextet created by hyperfine coupling of the $S = 2$ spin to ^{95,97}Mo ($I = {}^5/_2$, 25.5% total). **2**(**Mo**^{V}) also was chemically oxidized with $FcPF_6$ and gave spectra identical to those measured for **1**(**Mo**^{V}). The g values for **1**(**Mo**^{V}) and for **2**(**Mo**^{V}) (Table 3) are larger than those for $[Cp_2Mo^{V}Cl_2]^+$ and $[Cp_2Mo^{V}(O_2CPh)_2]^+$, which can be ascribed to the effect of delocalization onto the sulfurs. The 77 K spectrum of **1**(**Mo**^{V}) shows a typical rhombic signal with $g_1 = 2.026$, $g_2 = 2.019$, $g_3 = 1.993$, with an average value of $\langle g \rangle = 2.013$, which, within experimental error, is equal to the g_{iso} from the room-temperature spectrum.

The measured ^{95,96}Mo hyperfine coupling constant, $A = 22$ MHz for **1**(**Mo**^{V}) and for **2**(**Mo**^{V}), is about one-fifth that for the simple complexes, $[Cp_2Mo^{V}Cl_2]^+$ and $[Cp_2Mo^{V}(O_2CPh)_2]^+$, and more striking, less than half the value for $[Cp_2Mo(tdt)]^+$ [21] (Table 3). The diminished coupling constants for **1**(**Mo**^{V}) and for **2**(**Mo**^{V}) indicate that the dithiolatoporphyrazine delocalizes spin from the molybdocene moiety even better than the apparently similar $[Cp_2Mo(tdt)]^+$.

3(**Mo**^{IV},**Mo**^{IV}) can be titrated with ferrocenium hexafluorophosphate, to form first **3**(**Mo**^{V},**Mo**^{IV}) and then **3**(**Mo**^{V},**Mo**^{V}). The 77 K EPR spectra of frozen solutions of both the singly and doubly oxidized species are given in Figure 6, which also shows the 77 K EPR spectra of **1**(**Mo**^{V}) for comparison. As expected, **3**(**Mo**^{V},**Mo**^{IV}), which has one Mo^{V} ion, gives a spectrum identical to that measured for **1**(**Mo**^{V}). The spectrum

(19) Ehrlich, L. A.; Skrdla, P. J.; Jarrell, W.; Sibert, J. W.; Armstrong, N. R.; Saavedra, S. S.; Barrett, A. G. M.; Hoffman, B. M. *Inorg. Chem.* **2000**, *39*, 3963−3969.

(20) Lee, S.; White, A. J. P.; Williams, D. J.; Barrett, A. G. M.; Hoffman, B. M. *J. Org. Chem.*, **2001**, *66*, 461−465.

(21) Lindsell, W. E. *J. Chem. Soc., Dalton Trans.* **1975**, *23*, 2548−2552.

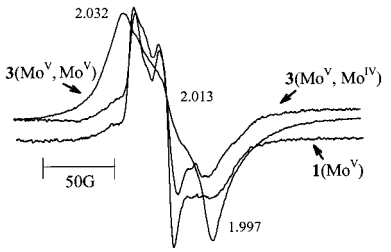

Figure 6. X-band, 77 K, EPR spectra of **3**(**Mo^{V},Mo^{IV}**), **3**(**Mo^{V},Mo^{V}**), and **1**(**Mo^{V}**) modulation amplitude = 5.0 G.

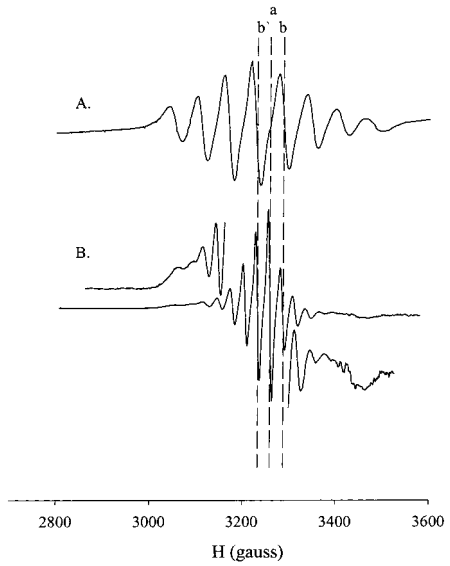

Figure 7. X-band, 298 K, EPR spectra of (A) **1**(**V^{IV}**) and (B) **3**(**V^{IV},V^{IV}**) and **4**(**V^{IV},V^{IV}**). The dashed lines are included to facilitate comparison between spectra A and B, which is hampered by the extreme line width variations in B. Outer dashed lines indicate fields from $M_I = -^7/_2$ and $+^7/_2$ for **1**(**V^{IV}**); dashed lines b and b′ indicate the $m_I = \pm^1/_2$ lines. They are seen to correlate with two lines, $m_I^t = m_I(1) + m_I(2) = \pm 1$, for B. Dashed line a corresponds to no line in A but to the $m_I^t = 0$ line in B.

for the doubly oxidized species, **3**(**Mo^{V},Mo^{V}**), is much broader, presumably due to dipole−dipole interactions between the two Mo^{V} centers.

(ii) Vanadocene pz's. The room-temperature X-band EPR spectrum for the solitaire vanadocene pz, **1**(**V^{IV}**) (Figure 7), exhibits the expected 8-line pattern for an $S = 2$ system with hyperfine coupling to a single ^{51}V ($I = ^7/_2$) nucleus. The hyperfine splitting constant of 60 G (169 MHz) matches values reported for other vanadocene dithiolene compounds.[15] The peaks do not have equal intensity because they are differentially broadened by motional effects; the high-molecular-weight pz has a relatively slow tumbling rate in solution (large τ_c). In this tumbling regime, the line widths (lw) follow the well-known relation, $lw = A + Bm_I + Cm_I^2$, where m_I represents the nuclear spin subcomponent of the transitions.[22]

The room-temperature X-band EPR spectra for the dinuclear pz's, **3**(**V^{IV},V^{IV}**) and **4**(**V^{IV},V^{IV}**) (Figure 7), do *not* exhibit the simple 8-line pattern for monomeric vanadium(IV) that is seen for **1**(**V^{IV}**) and that is expected if the two vanadocene units of a dinuclear complex are independent. Instead, **3**(**V^{IV},V^{IV}**) and **4**(**V^{IV},V^{IV}**) exhibit a striking 15-line pattern, which has the same breadth as the 8-line pattern seen for **1**(**V^{IV}**), but with additional lines "interpolated" between them, as shown in the figure.[23] This pattern indicates that exchange coupling between the vanadium centers[24] creates an $S = 1$ state. The $n = 2$ interacting vanadium nuclei ($I = ^7/_2$) give $2nI + 1 = 15$ hyperfine lines, but the breadth of the pattern is preserved because each electron spin is hyperfine-coupled only to its own nucleus by A_{iso}. As a result of this,[24] the effective dinuclear isotropic hyperfine coupling constant of **3**(**V^{IV},V^{IV}**) and **4**(**V^{IV},V^{IV}**), $A^{di}_{iso} = 30$ G (84 MHz), is exactly half the hyperfine coupling found for the mononuclear compound, **1**(**V^{IV}**) ($A_{iso} = 60$ G = 169 MHz). Spectra of frozen solutions of **3**(**V^{IV},V^{IV}**) and **4**(**V^{IV},V^{IV}**) show a strong "powder" signal that also displays splittings from $n = 2$ equivalent vanadium nuclei. As with the solution spectra, the hyperfine couplings are half those seen for **1**(**V^{IV}**), and thus the 77 K signal also is associated with the triplet state. The fluid solution data do not show whether exchange is ferromagnetic, with the triplet as ground state, or is antiferromagnetic with thermal population of the triplet, while the observation of a strong signal from the triplet state at 77 K is compatible with ferromagnetic coupling. However, only helium temperature experiments would be conclusive on this point. Regardless, these EPR results demonstrate that the porphyrazine macrocycle is capable of mediating exchange interactions between metals bound to the periphery of **4**(**V^{IV},V^{IV}**) at a V−V separation of 14.5 Å.

Conclusion

We have prepared and characterized a series of novel soluble molybdocene and vanadocene porphyrazines and obtained the X-ray structure of the trans divanadium pz, **4**(**V^{IV}, V^{IV}**). The molybdocene pz's are highly *redox-active*, and the Mo^{V} states show substantial delocalization by the pz ring. The electron spins of the two vanadium atoms of **3**(**V^{IV},V^{IV}**) and of **4**(**V^{IV},V^{IV}**) exhibit through-bond exchange coupling, though the vanadium atoms are separated by a metal−metal distance of 14.5 Å. The coupling will be far stronger when mediated by a metal ion incorporated within the pz core, and thus these results suggest that dithiolene-appended porphyrazines may be useful precursors for the preparation of *redox-switchable*, magnetically coupled supermolecular arrays.

Materials and Methods

Procedures. All starting materials were purchased from Aldrich Chemical and used as received, with the exception of the metallocene dichlorides ($MoCp_2Cl_2$ and VCp_2Cl_2), which were purchased from Strem Chemicals and used as received. THF was distilled from sodium/benzophenone ketyl, acetone was distilled from $CaSO_4$, and MeOH was distilled from CaH_2. All other solvents were used as purchased without additional purification. Anhydrous NH_3 (Linde Specialty Gases) was ultra-high-purity grade. Silica gel used for chromatography was Baxter silica gel 60 Å (230−400 mesh). Sodium metal was freshly cut under hexanes prior to use.

Bis(4-*tert*-butylphenyl)pyrroline (**5**),[8] 2,3-dipropylmaleonitrile **(6)**,[9] [(4-((butyloxy)carbonyl)benzyl)thio]maleonitrile ((**BCB**)$_2$mnt, **7**),[3,4] bis-(benzylthio)maleonitrile (**11**),[13] and **8** and **13**[8] were prepared as previously reported. Schlenk-line manipulations were performed on an apparatus purchased from Chemglass with all PTFE valves and with dry nitrogen ($CaSO_4$).

^{1}H and ^{13}C NMR spectra were obtained using either a Gemini 300 MHz, Mercury 400 MHz, or Inova 500 MHz spectrometer. Electronic absorption spectra were recorded using a Hewlett-Packard HP8452A diode array spectrophotometer. Cyclic voltammetry experiments were done at room temperature in methylene chloride with 0.1 M tetrabu-

(22) Weil, J. A.; Bolton, J. R.; Wertz, J. E. *Electron Paramagnetic Resonance: Elementary Theory and Practical Applications*; John Wiley & Sons: New York, 1994.

(23) Toward the edge of the pattern, this is somewhat obscured by differential broadening.

(24) Pilbrow, J. R. *Transition Ion Electron Paramagnetic Resonance*; Clarendon Press: Oxford, 1990.

tylammonium hexafluorophosphate as the supporting electrolyte using a Cypress Systems 2000 electroanalytical system. A platinum working electrode, a Ag/AgCl reference electrode, and an Ag wire counter electrode were used, with ferrocene added to the cell at the end of the experiment as an internal reference, unless otherwise noted. All $E_{1/2}$ values were calculated from $(E_{pa} + E_{pc})/2$ at a scan rate of 110 mV s^{-1} and no correction for junction potentials. Elemental analyses were preformed by Onieda Research Services (Whiteboro, NY). Fast atom bombardment mass spectra (FAB-MS), atmospheric phase chemical ionization mass spectra (APCI-MS), and electrospray mass spectra (ES-MS) were recorded locally by Dr. Doris Hung and Dr. Fenghe Qiu using a VG-70-250SE (FAB-MS) and a Micromass Quattro II RCMS triple-quadrupole (APCI-MS) instrument. Electron paramagnetic resonance (EPR) spectra were measured by using a modified Varian E-4 X-band spectrometer, with the field calibrated using diphenylpicryhydrazyl (dpph) as a standard.

Synthesis of H_2[Pz(SBCB)$_2$;B_3], B = (*n*-propyl)$_2$ (9). Magnesium metal (0.230 g, 9.46 mmol) and *n*-BuOH (90 mL) were heated to reflux under N_2. At reflux, a small chip of iodine was added to facilitate the formation of magnesium butoxide. After 12 h at reflux, 4.00 g (25 mmol) of 2,3-dipropylmaleonitrile (**6**)[9] and 1.84 g (3.5 mmol) of [(4-((butyloxy)carbonyl)benzyl)thio]maleonitrile ((BCB)$_2$mnt, **7**) were added to the butoxide mixture; the solution immediately turned a bright green color which developed into a dark blue color over the course of the reaction. After 24 h, the reaction was stopped and the BuOH was removed under reduced pressure; the remaining dark blue residue was dissolved in excess CF_3COOH (~50 mL).The solution was stirred for 15 min in the dark and then poured onto crushed ice and neutralized with concentrated NH_4OH. The dark blue solid was filtered and washed copiously with MeOH until the washings were colorless. The solid was filtered through a slurry of silica gel in chloroform. The filtrate was then purified by column chromatography (100% $CHCl_3$ eluant) (430 mg, 0.425 mmol, 12%): ^{1}H NMR (300 MHz, $CDCl_3$) δ 7.81 (d, J = 8 Hz, 4H), 7.42 (d, J = 8 Hz, 4H), 5.28 (s, 4H), 4.20 (t, J = 7 Hz, 4H), 3.93 (m, 8H), 3.78 (m, 4H), 2.28 (m, 12H), 1.63 (m, 4H), 1.28 (m, 4H), 1.24 (m, 18H), 0.88 (m, 6H); ^{13}C NMR (125 MHz, $CDCl_3$) δ 13.9, 15.2, 19.4, 25.6, 26.1, 28.4, 29.9, 30.9, 40.0, 62.6, 129.3, 129.5, 130.0, 141.2, 142.2, 142.3, 143.8, 146.2, 147.6, 158.2, 162.5, 162.8; UV−vis ($CHCl_3$) λ_{max} (log ϵ) 346 (4.63), 596 (4.48), 634 (4.50); HRMS (FAB-MS) *m*/*z* 1011.543 (M + H^+), calcd for $C_{58}H_{75}N_8S_2O_4$ 1011.535 Anal. Calcd for $C_{59}H_{75}N_8Cl_3O_4S_4$ (**9** + $CHCl_3$): C, 62.67; H, 6.68; N,9.91. Found: C, 63.28; H, 7.03; N, 10.16.

H_2[Pz(S_2MoCp$_2$;B_3)], B = (*tert*-butylphenyl)$_2$, 1(Mo^{IV}). Macrocycle **8** (0.200 g, 0.129 mmol) was put in a 50 mL three-neck round-bottomed flask, equipped with a coldfinger. The pz was cooled to −78 °C in an acetone/CO_2 bath, and ca. 30 mL of liquid NH_3 was added via the coldfinger. Sodium metal (0.030 g, 1.30 mmol), freshly cut under hexanes, was added followed by ca. 20 mL of THF to solubilize the mixture. The solution immediately turned a red-orange color, which progressed to a purple-cranberry color. After 1 h, the acetone/CO_2 bath was removed, and the solution was allowed to reflux through the coldfinger for 30 min. NH_4Cl (0.041 g, 0.774 mmol) was added to quench the excess sodium and sodium amide. The NH_3 and THF were vented off under a stream of N_2, yielding a dark green powder containing the disodium salt of the porphyrazine and NaCl. The dithiolate was not isolated, due its air sensitivity. The reaction residue was dissolved in deaerated acetone (40 mL). In a separate 100 mL Schlenck flask, Cp_2MoCl_2 and Cs_2CO_3 were suspended in deaerated acetone (40 mL). The pz^{2-} was transferred dropwise, via cannula, to the Cp_2MoCl_2 suspension and stirred for 12 h. The solvent was removed, and the pz was chromatographed on silica gel using CH_2Cl_2/hexane (80:20) as the eluant. The major teal green band was collected (0.80 g, 44% yield based on **8**): ^{1}H NMR (300 MHz, $CDCl_3$) δ 8.48 (m. 4H), 8.29 (m, 8H), 5.69 (s, 10H), 1.49 (s, 18H), 1.482 (s, 18H), 1.476 (s, 18H); UV−vis ($CHCl_3$) λ_{max} (log ϵ) 368 (4.85), 462 (4.35), 622 (4.95), 672 (sh) (4.44); HRMS (FAB-MS) *m*/*z* 1396.29 (M^+), calcd for $C_{86}H_{90}MoN_8S_2$ 1396.58. Anal. Calcd for $C_{86}H_{90}MoN_8S_2$: C, 74.00; H, 6.50; N, 8.03. Found C, 73.66; H, 6.10; N, 8.05.

H_2[Pz(S_2MoCp$_2$;B_3)], B = (*n*-propyl)$_2$, 2(Mo^{IV}). Macrocycle **9** (0.200 g, 0.198 mmol) was deprotected by the method described above for **8**. Due to the air sensitivity of the dithiolate, no attempt was made to isolate the product. The reaction residue containing **4b** was dissolved in deaerated acetone (40 mL). In a separate 100 mL Schlenck flask, Cp_2MoCl_2 and Cs_2CO_3 were suspended in deaerated acetone (40 mL). The pz^{2-} was transferred dropwise, via cannula, to the Cp_2MoCl_2 suspension and stirred for 12 h. The solvent was removed, and the pz was chromatographed on silica gel using $CHCl_3$ as the eluant. The major azure blue-green band was collected (0.60 g, 36% yield based on **9**): ^{1}H NMR (300 MHz, $CDCl_3$) δ 5.64 (s, 10H), 3.88 (m, 12H), 2.30 (M, 12H), 1.22 (m, 18H); UV−vis ($CHCl_3$) λ_{max} 346, 576, 637; HRMS (MALDI-TOF) *m*/*z* 856.298 (M^+), calcd for $C_{44}H_{54}N_8S_2Mo$ 856.297.

H_2[Pz(S_2MoCp$_2$;B_3)], B = (*tert*-butylphenyl)$_2$, 1(V^{IV}). Macrocycle **8** (0.100 g, 0.065 mmol) was deprotected by the method described above for the preparation of **1**(**Mo^{IV}**). The dithiolate was not isolated, due its air sensitivity. The reaction residue was dissolved in deaerated acetone (20 mL). In a separate 50 mL Schlenck flask, Cp_2VCl_2 was suspended in deaerated acetone (20 mL). The pz^{2-} was transferred dropwise, via cannula, to the Cp_2VCl_2 suspension and stirred for 12 h. The solvent was removed under vacuum, and the crude pz was taken into the glovebox and chromatographed on silica gel using toluene as the eluant. The major blue-green band was collected (0.30 g, 30% yield based on **8**): UV−vis ($CHCl_3$) λ_{max} 371, 459, 609, 684; FAB-MS *m*/*z* 1349 (M^+), calcd for $C_{86}H_{90}N_8S_2V$ 1349; EPR (X-band, 9.132 GHz), $\langle G\rangle_{rt}$ = 2.014, 8-line pattern, $\langle A_{iso}\rangle$ = 60 G (168 MHz).

H_2[Pz(S_2MoCp$_2$;B_3)]$^+$[PF_6]$^-$, B = (*tert*-butylphenyl)$_2$, 1(Mo^{V}). Macrocycle **1**(**Mo^{IV}**) (0.040 g, 0.029 mmol) was dissolved in ca. 10 mL of deaerated CH_2Cl_2. Ferrocenium hexafluorophosphate ($FcPF_6$) (0.020 g, 0.054 mmol) was dissolved in ca. 20 mL of deaerated CH_2Cl_2 and added, via a syringe, to the teal green pz solution, which changed to a dark green color, which was used without further purification: UV−vis (CH_2Cl_2) λ_{max} 371, 481, 622, 672; APCI-MS *m*/*z* 1397.7 (M + H^+), calcd for $C_{86}H_{90}N_8S_2Mo$ 1396.6; EPR (X-band, 9.132 GHz), ^{95,97}Mo, I = 5/2, 25.5%, $\langle G\rangle_{rt}$ = 2.010, 6-line pattern, $\langle A_{iso}\rangle$ = 8 G (22 MHz), $\langle G\rangle_{77\,K} - g_1$ = 2.024, g_2 = 2.018, g_3 = 1.998.

H_2[Pz(S_2MoCp$_2$;B_3)]$^+$[PF_6]$^-$, B = (*n*-propyl)$_2$, 2(Mo^{V}). Macrocycle **2**(**Mo^{IV}**) (0.030 g, 0.035 mmol) was dissolved in ca. 10 mL of deaerated CH_2Cl_2. Ferrocenium hexafluorophosphate ($FcPF_6$) (0.026 g, 0.070 mmol) was dissolved in ca. 20 mL of deaerated CH_2Cl_2 and added, via a syringe, to the teal green pz solution, which changed to a dark green color, which was used without further purification: UV−vis (CH_2Cl_2) λ_{max} 352, 601, 627; EPR (X-band, 9.132 GHz), ^{95,97}Mo, I = 5/2, 25.5%, $\langle G\rangle_{rt}$ = 2.009, 6-line pattern, $\langle A_{iso}\rangle$ = 8 G (22 MHz), $\langle G\rangle_{77\,K} - g_1$ = 2.026, g_2 = 2.019, g_3 = 1.993.

4,7-Bis(butyloxy)-1,3-diiminoisoindoline (10). Commercially available 3,6-dibutoxy-1,2-benzene dicarbonitrile (9.0 g, 33.1 mmol) was suspended in ethylene glycol (450 mL) in a 1 L three-necked round-bottom flask. Freshly cut Na (0.145 g) was added, and NH_3(g) was bubbled through the solution for ca. 1 h, after which time the mixture was heated to 150 °C under a positive pressure of N_2 for 5 h. During the course of the reaction, the solution turned from colorless to a yellow color. The hot solution was then poured into ice−water (1 L), and the precipitate which formed was filtered and recrystallized from MeOH to yield **8** (9.17 g, 31.7 mmol, 96% yield): ^{1}H NMR (300 MHz, $CDCl_3$) δ 0.97 (t, J = 8 Hz, 6H), 1.49 (m, 4H), 1.82 (m, 4H), 4.06 (t, J = 6 Hz, 4H), 6.91 (s, 2H), 8.1 (vbr, s, 3H); ^{13}C NMR (100 MHz, $CDCl_3$) δ 14.2, 19.6, 31.5, 68.9, 77.0, 77.3, 77.6, 116.3, 120.8, 149.4, 167.7; IR APCI-MS *m*/*z* 290.4 (M + H^+), calcd for $C_{16}H_{23}N_3O_2$ 289.2.

***trans*-H_2[Pz(*S*-benzyl$_2$)$_2$;B_2)], B = 3,6-dibutoxybenzene (12).** Magnesium metal (0.110 g, 4.53 mmol) and *n*-BuOH (35 mL) were heated to reflux under N_2. At reflux, a small chip of iodine was added to facilitate the formation of magnesium butoxide. After 12 h at reflux, the temperature was lowered to 100 °C, 2.40 g (8.3 mmol) of 4,7-bis-(butyloxy)-1,3-diiminoisoindoline (**8**) and 2.25 g (6.99 mmol) of bis-(benzylthio)maleonitrile (**9**) were added to the butoxide mixture, and the solution immediately turned a yellow-orange color which developed into a green color over the course of the reaction. After 5 h, the reaction was stopped, and the BuOH was removed under reduced pressure; the remaining green residue was dissolved in excess CF_3COOH (~50 mL).The solution was stirred for 15 min, in the dark, and then poured onto crushed ice and neutralized with concentrated NH_4OH. The green pz was extracted into CH_2Cl_2, dried over Na_2SO_4, and then purified by column chromatography (80:20 CH_2Cl_2/hexane) (0.157 g, 0.131 mmol,

8.3%): ^{1}H NMR (300 MHz, $CDCl_3$) δ 1.05 (t, $J = 7$ Hz, 12H), 1.75 (m, 8H), 2.18 (m, 8H), 4.58 (t, $J = 7.04$ Hz, 8H), 5.40 (s, 8H), 7.01 (m, 12H), 7.27 (m, 8H), 7.54 (s, 4H); ^{13}C NMR (125 MHz, CD_2Cl_3) δ 12.4, 19.8, 32.2, 39.8, 72.8, 118.3, 128.7, 129.2, 129.3, 131.6, 138.1, 139.4, 139.5, 151.2. 151.5; UV−vis (CH_2Cl_2) λ_{max} (log ϵ) 342 (5.37), 434 (4.99), 656 (5.42), 720 (5.10), 796 (5.34); APCI-MS *m*/*z* 1191.5 ($M + H^+$), calcd for $C_{68}H_{70}N_8O_4S_4$ 1190.4.

H_2[Pz(S_2MoCp$_2$)$_2$;B_2)], B = (3,6-dibutoxybenzene), 3(Mo^{IV},Mo^{IV}). Macrocycle **12** (0.099 g, 0.083 mmol) was deprotected via the method described above for the preparation of **3**(Mo^{IV},Mo^{IV}). The tetrathiolate was not isolated, due its air sensitivity. The reaction residue was dissolved in deaerated MeOH (40 mL). In a separate 100 mL Schlenck flask, Cp_2MoCl_2 and Cs_2CO_3 were suspended in deaerated MeOH (40 mL). The pz^{4-} was transferred dropwise, via cannula, to the Cp_2MoCl_2 suspension and stirred for 12 h. The solvent was removed, and the pz was chromatographed on silica gel using CH_2Cl_2/MeOH (90:10) as the eluant. The major azure blue-green band was collected (0.54 g, 51% yield based on **12**): ^{1}H NMR (300 MHz, CD_2Cl_2) δ 0.880 (t, $J = 7$ Hz, 12H), 2.025 (m, 8H), 2.043 (m, 8H), 4.619 (t, $J = 6$, 8H), 5.670 (s, 20H), 7.430 (s, 4H); UV−vis (CH_2Cl_2) λ_{max} (log ϵ) 312 (5.50), 344 (5.56), 622 (5.79), 670 sh (5.23); (FAB-MS) *m*/*z* 1282.0 (M^+), calcd for $C_{60}H_{62}N_8O_4S_4Mo_2$ 1282.2.

H_2[Pz(S_2VCp$_2$)$_2$;B_2)], B = 3,6-dibutoxybenzene, 3(V^{IV},V^{IV}). Macrocycle **12** (0.131 g, 0.110 mmol) was deprotected by the method described above for **3**(Mo^{IV},Mo^{IV}). The tetrathiolate was not isolated, due its air sensitivity. The reaction residue was dissolved in deaerated acetone (40 mL). In a separate 100 mL Schlenck flask, Cp_2VCl_2 (0.045 g, 0.179 mmol) was suspended in deaerated acetone (40 mL) The pz^{4-} was transferred dropwise, via cannula, to the Cp_2VCl_2 suspension and stirred for 12 h. The solvent was removed under vacuum, and the crude pz was taken into the glovebox and chromatographed on silica gel using toluene/acetone (90:10) as the eluant. The major blue band was collected (0.025 g, 19% yield based on 0.131 g of **12**): UV−vis λ_{max} 399, 610, 667, 742 (very broad); (FAB-MS) *m*/*z* 1189 ($M + H^+$), calcd for $C_{60}H_{62}N_8O_4S_4V_2$ 1188.3; X-band EPR spectrum (298 K, toluene) $g =$ 2.00, 15 lines, $a_{iso} = 30$ G.

H_2[Pz(S_2VCp$_2$)$_2$;B_2)], B = (*tert*-butylphenyl)$_2$, 4(V^{IV},V^{IV}). Macrocycle **13** (0.075 g, 0.043 mmol) was deprotected via the method described above for the preparation of **3**(Mo^{IV},Mo^{IV}). The tetrathiolate was not isolated, due its air sensitivity. The reaction residue was dissolved in deaerated acetone (40 mL). In a separate 100 mL Schlenck flask, Cp_2VCl_2 (0.022 g. 0.087 mmol) was suspended in deaerated acetone (40 mL). The pz^{4-} was transferred dropwise, via cannula, to the Cp_2VCl_2 suspension and stirred for 12 h. The solvent was removed under vacuum, and the crude pz was taken into the glovebox and chromatographed on silica gel using toluene/acetone (90:10) as the eluant. The major blue band was collected (0.014 g, 23% yield based on **13**): UV−vis λ_{max} 399, 610, 667, 742 (very broad); (FAB-MS) *m*/*z* 1329 ($M + H^+$), calcd for $C_{76}H_{74}N_8S_4V_2$ 1328; X-band EPR spectrum (298 K, toluene) $g = 2.00$, 15 lines, $a_{iso} = 30$ G.

H_2[Pz($S_2$$Mo^{V}Cp_2$;$S_2$$Mo^{IV}Cp_2$;$B_2$)]$^+$[$PF_6$]$^-$, B = 3,6-dibutoxybenzene, 3(Mo^{V},Mo^{IV}). 3(Mo^{IV},Mo^{IV}) (0.015 g, 0.018 mmol) was dissolved in ca. 10 mL of deaerated CH_2Cl_2. One milliliter of a 9.0 mM solution of ferrocenium hexafluorophosphate in 80:20 CH_2Cl_2/acetone was added to the pz. The solution, which turned from a teal green color to a dark green color, was used without further purification: UV−vis (CH_2Cl_2) λ 420, 625, 709, 809; EPR (X-band, 9.132 GHz), ^{95,97}Mo, $I = 5/2$, 25.5%, $\langle G\rangle_{77\,K} - g_1 = 2.024$, $g_2 = 2.018$, $g_3 =$ 1.998.

H_2[Pz($S_2$$Mo^{V}Cp_2$)$_2$;$B_2$)]$^{2+}$[$PF_6$]$_2^{2-}$, B = 3,6-dibutoxybenzene, 3-(Mo^{V},Mo^{V}). 17 (0.015 g, 0.018 mmol) was dissolved in ca. 10 mL of deaerated CH_2Cl_2. One milliliter of an 18.0 mM solution of ferrocenium hexafluorophosphate in 80:20 CH_2Cl_2/acetone was added to the pz. The solution initially turned from a teal green color to a dark green color, and then a dark green solid precipitated out. The solid was filtered and redissolved in 60:40 CH_2Cl_2/acetone and was used without further purification: UV−vis (CH_2Cl_2) λ 368, 418, 642, 708, 808; EPR (X-band, 9.132 GHz), ^{95,97}Mo, $I = 5/2$, 25.5%, $\langle G\rangle_{77\,K} - g_1 = 2.032$, $g_2 =$ 2.013, $g_3 = 1.997$.

X-ray Structure Determination. Platelike crystals of **4**(V^{IV},V^{IV}) were grown from acetone/MeOH in a nitrogen-filled NMR tube. Immediately prior to the X-ray experiment, these crystals were transferred to Paratone-N oil, and one crystal (0.17 × 0.17 × 0.20 mm) was mounted on a glass fiber. Data were collected on an Enraf Nonius CAD4 diffractometer with graphite-monochromated Mo Kα radiation at a temperature of -120 ± 1 °C using the $\omega-2\theta$ scan technique to a maximum 2θ value of 46.9°. The structure was solved by direct methods[25] and expanded using Fourier techniques[26] in the space group $P2_1/c$ (No. 14). Out of 6633 reflections collected, only 2143 were greater than 3σ, and considered "observed". Owing to the paucity of data, the vanadium and sulfur atoms were refined anisotropically, while the rest were refined isotropically. Hydrogen atoms were included in idealized positions, except those on the solvent molecules, but not refined. The final cycle of full-matrix least squares refinement (least-squares function minimized: $\sum w(F_o^2 - F_c^2)^2$, where $w = 1/[\sigma^2(F_o)] = [\sigma^2_c(F_o)] = [\sigma^2_c(F_o) + p^2F_o^2/4]^{-1}$; $\sigma_c(F_o)$ is the esd based on counting statistics and p is the p-factor) on F_2 was based on 2143 observed reflections and 228 variable parameters and converged (largest parameter shift was 0.01 times its esd) with unweighted and weighted agreement factors of R1 = 0.143 and wR2 = 0.239. The standard deviation of an observation of unit weight was 1.75. The weighting scheme was based on counting statistics. The maximum and minimum peaks on the final difference Fourier map corresponded to 1.18 and -0.74 e$^-$/Å^3, respectively, and were located in the *tert*-butyl and vanadium positions. Neutral atom scattering factors were taken from Cromer and Waber.[27] Anomalous dispersion effects were included in F_{calc}; the values for $\Delta f'$[1] and $\Delta f''$[11] were those of Creagh and McAuley.[28] The values for the mass attenuation coefficients are those of Creagh and Hubbell.[29] All calculations were performed using the teXsan for Windows version 1.05 crystallographic software packages from Molecular Structure Corp.

Acknowledgment. This work has been supported by the NSF (Grant CHE-9729590) and the Materials Research Center of Northwestern University. We thank Dr. Peter Doan for help with some of the EPR experiments and for helpful discussions.

Supporting Information Available: Crystal data, structure refinement, and tables of positional parameters, bond distances, bond angles, and anisotropic displacement parameters (PDF). This material is available free of charge via the Internet at http://pubs.acs.org.

JA003702X

(25) Sheldrick, G. M. In *Crystallographic Computing 3*; Sheldrick, G. M., Krüger, C., Goddard, R., Eds.; Oxford University Press: London, 1985; pp 175−189.

(26) Beurskens, P. T.; Admiraal, G.; Beurskens, G.; Bosman, W. P.; de Gelder, R.; Israel, R.; Smits, J. M. M. *The DIRDIF-94 Program System*; Technical Report of the Crystallography Laboratory; University of Nijmegen: The Netherlands, 1994.

(27) Cromer, D. T.; Waber, J. T. In *International Tables for X-ray Crystallography*; Ibers, J. A., Hamilton, W. C., Eds.; Kynoch Press: Birmingham, England, 1974; Vol. IV, pp 72−98.

(28) Creagh, D. C.; McAuley, W. J. In *Table 4.2.6.8;* Wilson, A. J. C., Ed.; Kluwer Academic Publishers: Boston, 1992; pp 219−222.

(29) Creagh, D. C.; Hubbell, J. H. In *Table 4.2.4.3*; Wilson, A. J. C., Ed.; Kluwer Academic Publishers: Boston, 1992; pp 200−206.